

# Assessment of cerebrovascular dysfunction after traumatic brain injury with fMRI and fNIRS

Franck Amyot<sup>a,b,\*</sup>, Kimbra Kenney<sup>a,b</sup>, Emily Spessert<sup>a,b</sup>, Carol Moore<sup>a,b</sup>, Margalit Haber<sup>c</sup>, Erika Silverman<sup>c</sup>, Amir Gandjbakhche<sup>d</sup>, Ramon Diaz-Arrastia<sup>b,c</sup>

<sup>a</sup> Department of Neurology, Uniformed Services University of the Health Sciences, 4301 Jones Bridge Road, Bethesda, MD 20814, USA

<sup>b</sup> Center for Neuroscience and Regenerative Medicine, Department of Neurology, Uniformed Services University of the Health Sciences, 4301 Jones Bridge Road, Bethesda, MD 20814, USA

<sup>c</sup> Department of Neurology, University of Pennsylvania Perelman School of Medicine, Philadelphia

<sup>d</sup> Section on Analytical and Functional Biophotonics, Eunice Kennedy Shriver National Institute of Child Health and Human Development (NICHD), National Institutes of Health (NIH), Bethesda, Maryland, USA

## ARTICLE INFO

### Keywords:

Near-infrared spectroscopy  
Functional magnetic resonance imaging  
Traumatic brain injury (TBI)  
Cerebrovascular reactivity (CVR)  
Hypercapnia

## ABSTRACT

Traumatic cerebral vascular injury (TCVI) is a frequent, but under-recognized, endophenotype of traumatic brain injury (TBI). It likely contributes to functional deficits after TBI and TBI-related chronic disability, and represents an attractive target for targeted therapeutic interventions. The aim of this prospective study is to assess microvascular injury/dysfunction in chronic TBI by measuring cerebral vascular reactivity (CVR) by 2 methods, functional magnetic resonance imaging (fMRI) and functional Near InfraRed Spectroscopy (fNIRS) imaging, as each has attractive features relevant to clinical utility.

42 subjects (27 chronic TBI, 15 age- and gender-matched non-TBI volunteers) were enrolled and underwent outpatient CVR testing by 2 methods, MRI-BOLD and fNIRS, each with hypercapnia challenge, a neuropsychological testing battery, and symptom survey questionnaires.

Chronic TBI subjects showed a significant reduction in global CVR compared to HC ( $p < 0.0001$ ). Mean CVR measures by fMRI were  $0.225 \pm 0.014$  and  $0.183 \pm 0.026$  %BOLD/mmHg for non-TBI and TBI subjects respectively and  $12.3 \pm 1.8$  and  $9.2 \pm 1.7$  mM/mmHg by fNIRS for non-TBI versus TBI subjects respectively. Global CVR measured by fNIRS imaging correlates with results by MRI-BOLD ( $R = 0.5$ ). Focal CVR deficits seen on CVR maps by fMRI are also observed in the same areas by fNIRS in the frontal regions.

Global CVR is significantly lower in chronic TBI patients and is reliably measured by both fMRI and fNIRS, the former with better spatial and the latter with better temporal resolution. Both methods show promise as non-invasive measures of CVR function and microvascular integrity after TBI.

## 1. Introduction

Traumatic brain injury (TBI) is a leading cause of death and disability around the world, and affects adults and children across all socioeconomic strata (Langlois et al., 2006). In the US, head trauma is responsible for 2.8 million emergency visits, 300,000 hospitalizations, and 50,000 deaths each year (Taylor et al., 2017). Traumatic cerebrovascular injury (TCVI) is one of the most common abnormalities acutely reported in TBI patients, including mild TBI (Yuh et al., 2013; Bartnik-Olson et al., 2014; Tong et al., 2004). Neuropathology studies in patients who die with TBI uniformly find evidence of microvasculopathy (Tomlinson, 1970; Graham et al., 2002; Stein et al., 2002;

Rodriguez-Baeza et al., 2003), a finding which is also noted in the few pathologic studies which have focused on patients with mild TBI (Oppenheimer, 1968; Blumbergs et al., 1995). Established neuroimaging methods enable quantitative measurement of cerebral blood flow (CBF) and cerebrovascular reactivity (CVR) in animals and humans (Kassner and Roberts, 2004; Yezhuvath et al., 2009; Chassidim et al., 2013). Finally, TCVI is an attractive target for therapeutic intervention, as established pharmacologic and non-pharmacologic therapies with proven efficacy in improving vascular health are already available (Shlosberg et al., 2010). Such therapies include phosphodiesterase-5 inhibitors (Li et al., 2007), 3-hydroxy-3-methyl-glutaryl-coenzyme A reductase inhibitors (Wu et al., 2011), angiotensin II receptor blockers

\* Corresponding author at: Center for Neuroscience and Regenerative Medicine, Department of Neurology, Uniformed Services University of the Health Sciences, 4301 Jones Bridge Road, Bethesda, MD 20814, USA.

E-mail address: [franck.g.amyot.civ@mail.mil](mailto:franck.g.amyot.civ@mail.mil) (F. Amyot).

<https://doi.org/10.1016/j.nicl.2019.102086>

Received 31 January 2018; Received in revised form 7 November 2019; Accepted 9 November 2019

Available online 11 November 2019

2213-1582/ © 2019 Published by Elsevier Inc. This is an open access article under the CC BY-NC-ND license (<http://creativecommons.org/licenses/by-nc-nd/4.0/>).

(Villapol et al., 2015), erythropoietin (Zhang et al., 2006) transforming growth factor beta (TGF $\beta$ ) inhibitors (Shlosberg et al., 2010), aerobic exercise (Pereira et al., 2007), dietary interventions (Scrimgeour and Condlin, 2014), and nutraceuticals such as omega-3 fatty acids (Hasadsri et al., 2013). The ready availability of these therapies highlights the need for reliable tools to measure TCVI noninvasively and sequentially.

CBF has been extensively studied after TBI in humans, mostly in the acute period within a few days of injury (Furuya et al., 2003; Menon, 2006), but several studies have looked at CBF weeks to years after TBI. There is a consistent body of literature in humans indicating that deficits in CBF are common after TBI (Bonne et al., 2003). Studies using single photon emission computed tomography (SPECT) (Bonne et al., 2003; Barkai et al., 2004; Lewine et al., 2007) and arterial spin labeling (ASL) (Kim et al., 2010; Kim et al., 2012) reveal alterations in global and regional resting CBF in TBI patients of all severities.

Well-established methods also exist to study CVR non-invasively in humans, after stimuli such as hypercapnia, breath holding, or acetazolamide (Kassner and Roberts, 2004). Transcranial Doppler (TCD), near infra-red spectroscopy (NIRS) and Magnetic Resonance Imaging (MRI) are the most popular methods in recent studies (Bailey et al., 2013; Gardner et al., 2015) particularly in subjects who had experienced the TBI exposures. Functional near Infra-Red Spectroscopy (fNIRS) has been used to study CVR after TBI as well as in other neurologic conditions (Lee et al., 2009; Rodriguez Merzagora et al., 2014; Zweifel et al., 2010a,b). Changes in CBF and associated changes in tissue concentrations of oxy- and deoxy-hemoglobin are measured by fNIRS (Kainerstorfer et al., 2014). Like TCD, fNIRS offers a very high temporal resolution, and while spatial resolution is superior to TCD, it is not as high as fMRI. fNIRS allows for reliable CVR measurements over time during dynamic challenges that are independent of hemoglobin concentration, skull thickness and extracranial circulation (Zweifel et al., 2010a; Diedler et al., 2011; Kainerstorfer et al., 2015). fNIRS has also been carried out in the chronic stage of TBI, and CVR abnormalities correspond to performance on the cognitive tests (Rodriguez Merzagora et al., 2014; Chernomordik et al., 2016).

Our group has recently reported that CVR assessed by measuring the response of the blood oxygen level dependent (BOLD) signal to hypercapnia is reduced in chronic TBI (Kainerstorfer et al., 2015). The pattern of CVR decline noted was not diffusely symmetric, but rather multifocal. Since MRI is expensive, time consuming, non-portable, and not well suited for use in emergency departments, critical care units, and outpatient clinics, the purpose of this study is to determine how the cerebrovascular response to hypercapnia measured with NIRS correlates with measures obtained using MRI-BOLD. The ability to inexpensively and repeatedly assess CVR in brain injured patients has high potential as a biomarker of TCVI.

## 2. Materials and method

### 2.1. Subjects

Adults (between 18 and 55 years) were consented and co-enrolled under 2 internal review board approved protocols (ClinicalTrials.gov NCT01762475 and NCT01789164). Inclusion criteria for TBI subjects included: TBI from 6 months to 10 years' prior with either Glasgow Coma Score between 3 and 12, post-traumatic amnesia > 24 h, or acute TBI-related neuroimaging abnormality (Computed Tomography (CT) or MRI). Exclusionary criteria included penetrating TBI, pre-existing disabling neurologic or psychiatric disorder, pregnancy, or unstable pulmonary or vascular disorder. Gender and age-matched individuals with no history of TBI, pre-existing disabling neurological or psychiatric disorders or pregnancy were enrolled as healthy controls (HC).

**Table 1**

Demographics, TBI characteristics, and neurobehavioral symptom survey analysis. BSI global is defined as the sum of BSI vestibular, BSI somatic, BSI depression and BSI anxiety. TBI = traumatic brain injury; HC = healthy control; STD = standard deviation; IQR = interquartile range (25th and 75th); LOC = loss of consciousness; GOS-E = Glasgow Outcome Scale-Extended.

	TBI (n = 27)	HC (N = 15)	P
Age, mean (std)	38.1 (10.9)	38.2 (7.4)	0.98
Gender (%male)	74	73	
Education, mean (std)	15.1 (2.8)	16.7 (5.1)	0.08
Time since TBI (month), median (IQR)	25 (14, 41)		
LOC > 30 min (%)	54		
Abnormal images (%)	87.5		
Days in ICU (days), median (IQR)	6 (3, 14)		
GOS-E, median (IQR)	7 (6, 7)		
BSI (total), median (IQR)	3 (1.5, 4.7)	0.25 (0, 1)	<0.001
BSI Vestibular, median (IQR)	0 (0, 2)	0 (0, 0)	0.003
BSI Somatic, median (IQR)	3 (2, 4)	0 (0, 2)	0.001
BSI Cognitive, median (IQR)	2 (0.25, 7)	0 (0, 0.75)	0.005
BSI Affective, median (IQR)	4 (0, 7)	0 (0, 1)	0.005

### 2.2. Demographics

42 (27 TBI and 15 HC) age and gender-matched subjects were consented, enrolled in the study and had data available for analysis (Table 1). They had a mean age of  $37.7 \pm 16$  years (range 20–55). TBI subjects were enrolled a median of 25 months post-injury. The majority of TBIs occurred as a result of traffic incidents. All but 2 subjects had TBI-related neuroimaging findings on initial cranial computerized tomography (CT), with hematomas and contusions the most common abnormality. Two subjects with initially normal CT scans had TBI-related structural abnormalities identified in the chronic state by the study MRI. All TBI subjects were hospitalized, stayed a median of 3 days in the intensive care unit (ICU) and over half received either inpatient or outpatient rehabilitation for their injury. At enrollment the median Extended Glasgow Outcome Scale (GOS-E) score was 7 (range 4–8) and the majority (77%) had persistent symptoms that met DSM-IV criteria for persistent post-concussive syndrome. On structural MRI, 15 showed focal encephalomalacia with or without microhemorrhage, 5 focal microhemorrhage only, 1 chronic subdural and 6 were normal, with either no evidence of trauma or resolution of earlier CT-evident subdural or subarachnoid hemorrhages. Four subjects had volume loss or global atrophy. 15 had visible encephalomalacias. In the frontal cortex, 18 subjects have focal encephalomalacia or microhemorrhage. All subjects underwent hypercapnia challenge twice (with both MRI-BOLD and NIRS) without adverse effect. The Table 1 summarizes the demography features of our population.

### 2.3. Hypercapnia

Each participant underwent MRI-BOLD and fNIRS sequences with CVR hypercapnia measurements according to the methods developed previously (Yezhuvath et al., 2009; Amyot et al., 2017; Wassermann et al., 2018). Hypercapnia was induced via a Douglas bag alternating between a flow of room air and 5% CO<sub>2</sub> mixed with room air every minute for 7 min total while the MRI-BOLD or fNIRS images were acquired. A long hypercapnia condition (60 s) was chosen to allow EtCO<sub>2</sub> pressure to reach a plateau before switching to Room air condition (Yezhuvath et al., 2009). End-tidal CO<sub>2</sub> (EtCO<sub>2</sub>) was measured continuously using a capnograph (Smith Medical, Model 9004). These conditions (5% CO<sub>2</sub> for no longer than one minute at a time) did not result in significant changes in mean arterial blood pressure, heart rate or oxygen saturation (Zhu et al., 2013).

2.4. MRI

*Scan:* MRI was performed on a Siemens Biograph mMR, fully integrated 3T MRI/PET. Whole-brain T1-weighted 1 mm isotropic structural scans were collected using a 3D multiecho MPRAGE sequence (176 sagittal slices, 256 mm FoV, TR 2530 ms, TI 1200 ms) Fluid-attenuated inversion recovery (FLAIR) images were acquired with the following parameters: TR/TE = 9090/112 ms, inversion time = 2450 ms, voxel size:  $0.9 \times 0.9 \times 3 \text{ mm}^3$ .

The 7 min hypercapnia challenge was done under an fMRI sequence: TR/TE = 2000/25 msec, flip angle =  $80^\circ$ , field of view =  $220 \times 220 \text{ mm}^2$ , matrix =  $64 \times 64$ , 36 slices, thickness = 3.6 mm, no gap between slices, 210 volumes.

*fMRI analysis:* The BOLD response signal is delayed from the EtCO<sub>2</sub> (Yezhuvath et al., 2009, 2012) which correspond to the time needed for the blood to travel between the lungs to the cerebrovascular network. The EtCO<sub>2</sub> time delay is individually time shifted (with one sec step increment) to achieve the maximum correlation with the BOLD response signal. We processed voxel-by-voxel CVR maps using a general linear model, with the shifted EtCO<sub>2</sub> time course as the regressor to generate CVR maps (in the units of % BOLD change/mmHg CO<sub>2</sub> change,%/mmHg) for each subject. Lu et al. previously described the full method (Lu et al., 2014). As preprocessing step, images were spatially realigned and re-sliced to correct for head motion with SPM (realign and re-slice toolbox) and a 6 mm (FWHM) Gaussian kernel was used for smoothing the resultant time series. As post processing steps, the CVR and FLAIR images were each co-registered with the MPRAGE images using SPM12.

2.5. fNIRS

*Scan:* We used a continuous wave fNIRS system (fNIRS Devices LLC, MD). The instrument consists of an array of four sources and 10 detectors, with a total of 16 source-detector pairs (see Fig. 1). In this system all sources and detectors are molded together in a single silicon band. It collects data at two wavelengths—730 and 850 nm—with an acquisition frequency of 2 Hz. The sensor band was positioned on patient's forehead covering the prefrontal cortex (PFC) area (dorsal and inferior frontal cortical areas) (Ayaz et al., 2012). The rigid montage is carefully position above the eyebrow and in the middle of the forehead. The first detector row is approximately at 3.5 cm above the nasion. This system was selected for this feasibility study because it is comfortable and easy to wear.

*fNIRS analysis:* NIRS light intensities at two wavelengths were then converted to changes in oxy-hemoglobin (HbO) and deoxy-hemoglobin (HbR) using the modified Beer-Lambert (MBLL) law (Delpy et al., 1988).

Processing of the raw NIRS signal involved detection and removal of artifacts related to subject motion as well as respiration and heart rate. We used both median filtering and the sliding window motion artifact rejection (SMAR) to detect and remove motion artifact and saturated

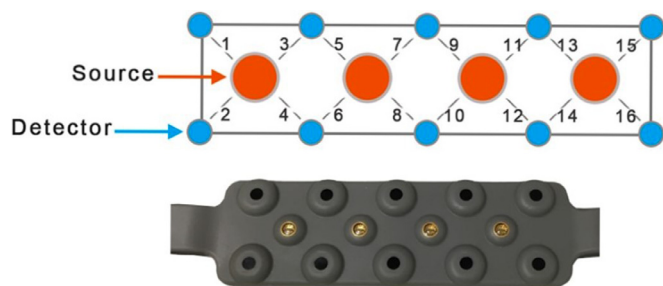


Fig. 1. Optical sensor pad schematic. It is composed of 4 sources and 10 detectors which form 16 source/detector pairs separated by 2.5 cm. The sensor pad is positioned on the volunteer's forehead.

channels (Ayaz et al., 2010). This algorithm uses presence of sharp spikes and high standard deviations of the signal ( $>3\%$  temporally) to detect motion. Correlation Based Signal Improvement was also used to remove any unidirectional changes in HbO and HbR signals (Ayaz, 2010; Cui et al., 2010). Then, a low pass frequency filter ( $<0.1 \text{ Hz}$ , Hanning window, order 20) was applied to remove high frequency contamination related to heart beat and respiration (Naseer, 2013; Kreplin and Fairclough, 2013; Izzetoglu et al., 2007). Afterward, signals were detrended to eliminate the slow changes in the signal.

The hemodynamic response is time delayed from the EtCO<sub>2</sub> and, like the fMRI analysis, the temporal EtCO<sub>2</sub> trace needs to be individually shifted with one step increment to achieve the maximum correlation with the hemoglobin signals. The time shift between the oxygenation (HbO – HbR) and EtCO<sub>2</sub> was also measured. CVR values for each channel is the solution of the linear equation between HbO (or HbR) and EtCO<sub>2</sub> using the Cholesky decomposition in MATLAB.

3. Results

3.1. CVR in healthy control

The inhalation of 5% CO<sub>2</sub> during 60 s is accompanied by an increase of EtCO<sub>2</sub> pressure measured by capnography. At baseline, the mean EtCO<sub>2</sub> value is  $39.9 \pm 1.6 \text{ mmHg}$  and rises to  $49 \pm 1.2 \text{ mmHg}$ . With fMRI, the EtCO<sub>2</sub> trace is followed by an increase of BOLD signal (Fig. 2-a). With fNIRS, the EtCO<sub>2</sub> trace is also followed by an increase of HbO and a decrease of HbR (Fig. 2-b). In average, in our healthy control group, the increase of HbO appears  $2.3 \pm 2.6 \text{ s}$  before the decrease of

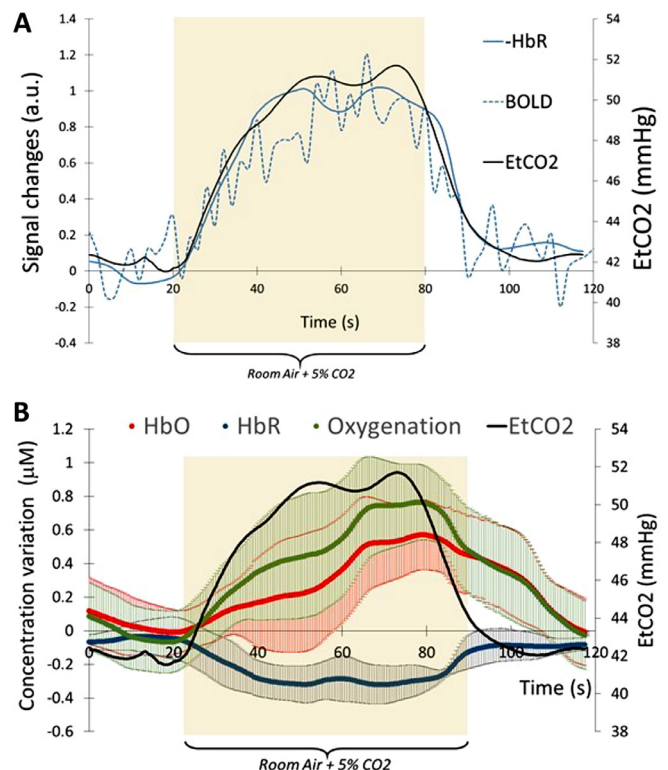


Fig. 2. A) Average of 3 time course of EtCO<sub>2</sub>, BOLD signal and deoxy-hemoglobin (HbR). BOLD signal and HbR were normalized with their relative maximum to their baseline. The EtCO<sub>2</sub> and HbR were time shift to match EtCO<sub>2</sub> trace. During the time range of 20 s–80 s, subject was breathing room air enriched with 5% CO<sub>2</sub>. BOLD signal and HbR signals were normalized with their respective maximum. B) Average of 3 time course of oxy-Hemoglobin (HbO), deoxy-Hemoglobin and oxygenation. The error bar represent the standard deviation for the 16 channels.

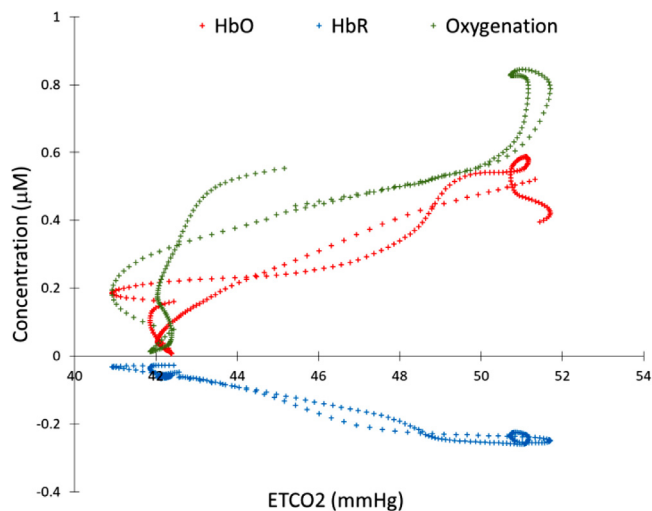


Fig. 3. Relationship between EtCO<sub>2</sub> and the time shifted fNIRS signal (HbO, HbR and Oxygenation). CVR is defined as the linear correlation between EtCO<sub>2</sub> trace and each fNIRS signal.

HbR. Because of this delay between HbO and HbR, the time shift between EtCO<sub>2</sub> trace and HBO signal is not the same as the time shift between EtCO<sub>2</sub> trace and HbR signal.

With the temporal EtCO<sub>2</sub> trace correctly shifted to match the HbO, oxygenation or HbR variation, we can measure the correlation between these parameters. Fig. 3 shows an example of linear relationship between HBO/HbR and the EtCO<sub>2</sub> trace.

With the appropriate temporal shift, we can measure the Pearson correlation between the EtCO<sub>2</sub> and the HbO, HbR, oxygenation, as well as between the EtCO<sub>2</sub> from MRI and the MRI BOLD signal for our healthy control group. BOLD signal and fNIRS signals are highly correlated with EtCO<sub>2</sub> trace (Pearson's correlation of 0.92, 0.94, -0.98 and 0.91 for BOLD, HbO, HbR and oxygenation,  $p < 0.0001$ )

We measured CVR for 17 healthy volunteers to investigate the CVR variability between subjects and also between different channels within the same subject. For each source/detector pair, we calculated the CVR from HbO, HbR but also from the difference between both parameters (oxygenation = HbO-HbR). In healthy volunteers, the CVR values were  $13.1 \pm 4.7 \mu\text{M}/\text{mmHg}$  using HbO as the parameter,  $-14.6 \pm 10.2 \mu\text{M}/\text{mmHg}$  using HbR and  $12.4 \pm 3.7 \mu\text{M}/\text{mmHg}$  using oxygenation (Table 2). We also analyzed the variability between the channels within the same individual. On average, the variability of CVR assessed by oxygenation was lowest (35%) and appears to be the best parameter to investigate CVR in fNIRS. Thus, we used oxygenation to quantify CVR among HC and TBI patient.

### 3.2. CVR in TBI

CVR values are significantly lower in the TBI group than the HC group, by both methods, fMRI and fNIRS (Fig. 4). With fMRI, mean CVR value is  $0.225 \pm 0.014 \text{ \%BOLD}/\text{mmHg}$  in HC and  $0.183 \pm 0.026 \text{ \%BOLD}/\text{mmHg}$  in TBI ( $p < 0.0001$ ). With fNIRS, mean CVR value is  $12.3 \pm 1.8 \mu\text{M}/\text{mmHg}$  in HC and  $9.2 \pm 1.7 \mu\text{M}/\text{mmHg}$  in TBI ( $p < 0.0001$ , effect size = 0.87).

In Fig. 5, sample CVR results using both fNIRS and fMRI are

**Table 2**  
Inter-subject and inter-channel variability of CVR values for 15 HC.

	Mean	Standard deviation	Variability between channels
HBO	13.1	4.7	41%
HBR	-14.6	10.2	85%
OXYGENATION	12.4	3.7	30%

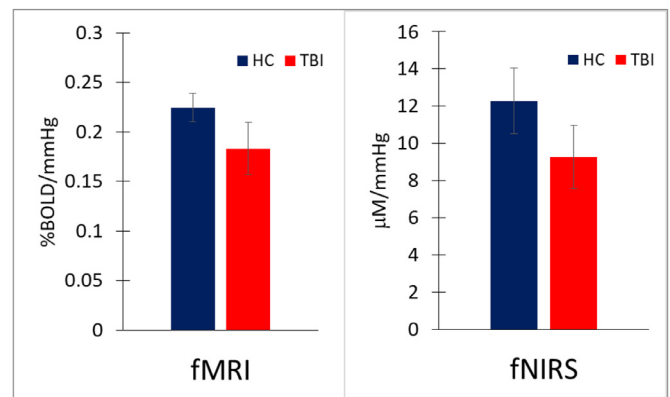


Fig. 4. Mean and standard deviation of CVR for HC and TBI group with the 2 modalities. With fMRI, mean CVR value is  $0.225 \pm 0.014 \text{ \%BOLD}/\text{mmHg}$  in HC and  $0.183 \pm 0.026 \text{ \%BOLD}/\text{mmHg}$  in TBI ( $p < 0.00001$ , effect size = 0.81). With fNIRS technique, mean CVR values is  $12.3 \pm 1.8 \mu\text{M}/\text{mmHg}$  in HC and  $9.2 \pm 1.7 \mu\text{M}/\text{mmHg}$  in TBI ( $p < 0.00001$ , effect size = 0.87).

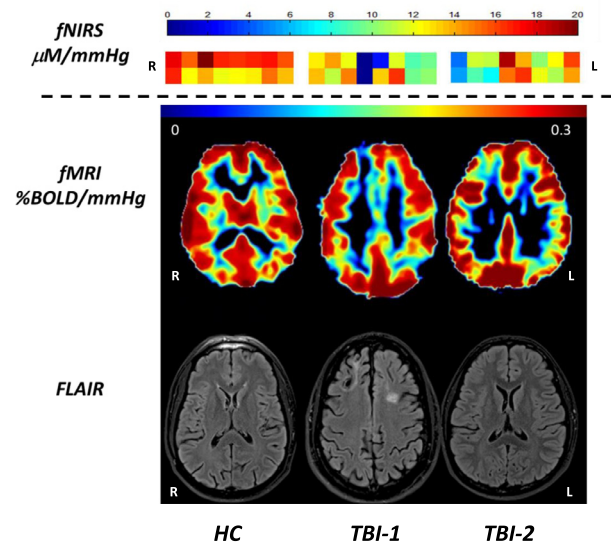
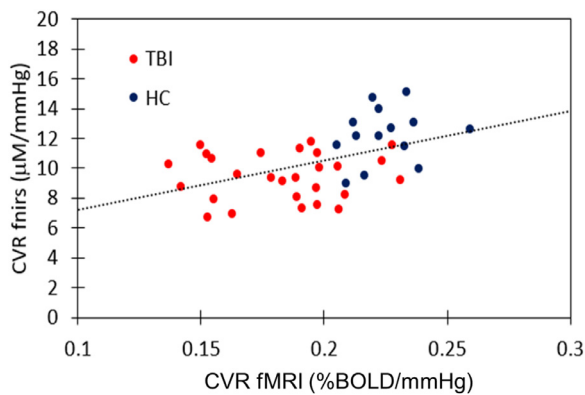


Fig. 5. CVR maps with fNIRS and fMRI modality and FLAIR map for one control (left column) and 2 TBI subjects (middle and right columns). The control subject shows a uniform CVR values with fNIRS and in the gray matter in fMRI. TBI-1 has a visible lesion (encephalomalacia) in the right prefrontal cortex on the FLAIR image and the lesion is also visible in CVR map (decreased CVR values) in fMRI and fNIRS. TBI-2 has no visible lesion on the FLAIR image, but a focal vascular lesion on the CVR map in fMRI (right prefrontal cortex). The decrease of CVR in fMRI is also visible with fNIRS.

compared in one HC and two TBI subjects. For each patient, the structural FLAIR image is co-registered with the CVR<sub>fMRI</sub>. HC presents a symmetric, uniformly distributed CVR<sub>fMRI</sub> map between the two hemispheres with high CVR values in the gray matter. However, in TBI-1, focal areas of encephalomalacia are visible in the frontal region by FLAIR imaging. This focal lesion is associated with lower CVRs value by both fMRI and fNIRS. TBI-2 is an example of a TBI patient without a visible structural lesion on FLAIR imaging. However, CVR<sub>fMRI</sub> values are low in the left frontal region, indicating a focal vascular dysfunction. This low CVR is also present in the CVR<sub>fNIRS</sub> map with values under  $8 \mu\text{M}/\text{mmHg}$ . In these two TBI patients, lesions in the frontal cortex can be detected and quantified equally by either fNIRS or fMRI.

In Fig. 6, we plotted for each individual global CVR values acquired with fMRI (x-axis) versus CVR values via fNIRS (y-axis). We see a moderate correlation between the two modalities with a Pearson's correlation of 0.47 ( $p = 0.001$ ).



**Fig. 6.** Correlation between the global CVR measured with fMRI and CVR measured with fNIRS (from the oxygenation data) for each subject. The red dot represent subject from the TBI group and the blue dot are subject for the HC group. The Pearson's correlation between the two modalities is  $R = 0.47$  ( $p = 0.001$ ).

## 4. Discussion

### 4.1. CVR in healthy volunteers

In this study, we were able to measure and quantify CVR with two different imaging modalities, fNIRS and fMRI, in a cohort of HC and chronic moderate-severe TBI subjects. CVR measures with fNIRS can be reliably obtained from HbO, HbR or a combination of both (oxygenation = HbO-HbR). The inter-channel variations in CVR and the inter-subject's variation in CVR were the lowest with the oxygenation signal. The variation of HbO and HbR signal between patients during hypercapnea were also noticed in Sleb's paper (Selb et al., 2014) with a contrast to noise ratio (CNR) lower than 1. In our study, CNR for the HC group is 3.0 for HbO, 2.6 for HbR and 3.1 for oxygenation. This difference can be explained by a longer hypercapnia duration in our study (60 s) than that used in the previous report. Indeed, the EtCO<sub>2</sub> graph (Fig. 2) shows that a plateau is reached after 30 s, which suggests that a period of 30 s, as used with Sleb's study, seems insufficient to reach a full CVR response. Also, with fMRI, several studies used a long hypercapnia period to study CVR with interval step changes of 60 s (Yezhuvath et al., 2012), 120 s (Mutch et al., 2014; Mutch et al., 2016) and 440 s (Yezhuvath et al., 2009) without high inter-subject variability in the whole CVR (Yezhuvath et al., 2009). Our fNIRS and fMRI results also suggest that a moderate (5% CO<sub>2</sub>) and longer duration hypercapnic challenge (60 s or longer) is needed to observe a change of blood flow. Our moderate CO<sub>2</sub> concentration can explain why Virtanen et al. (2009) didn't observe a significant HbO or HbR response to a 2% and 3% CO<sub>2</sub> increase with an estimated CNR lower than 1 for HbO and HbR.

The goal of our study was to identify vascular lesions, via CVR, in TBI patients with fNIRS and compare it with measures obtained using MRI-BOLD. BOLD signal is known to better fit HbR than HbO and a true comparison of the two techniques should only be done with HbR (Cui et al., 2011; Huppert et al., 2006). However with the increase of HbO and the decrease of HbR during our challenge, we found the best discriminating parameter is the difference between the two signals. HbT (HbO + HbR) or SO<sub>2</sub> (HbO/HbT) are also two parameters frequently used (Alderliesten et al., 2014) to quantify blood change, but they usually have a high CNR.

Moreover, the response of hypercapnia should be correlated with the EtCO<sub>2</sub> trace to measure the individual response to CVR. Even if the variability of EtCO<sub>2</sub> trace between patients is low, the range of amplitude of EtCO<sub>2</sub> between room air and 5% CO<sub>2</sub> varies between 8 and 11 mmHg, which can induce a high variability in hemodynamic response. In our study, the hemodynamic signal is normalized with EtCO<sub>2</sub> trace and it can be a reason for our low inter-subject variability.

### 4.2. CVR in TBI

CVR is a biomarker for vascular injury after TBI (Amyot et al., 2017; Kenney et al., 2016), which is more sensitive in discriminating TBI subjects from HC than CBF. While CVR with fMRI has already been studied (Amyot et al., 2017; Mutch et al., 2014), this is the first time CVR was measured with fNIRS in TBI. Both modalities were able to distinguish CVR abnormalities between the two groups.

While nearly all TBI subjects had abnormalities detectable on structural imaging (MPRAGE, FLAIR), most of the regions of low CVR appeared in normal-appearing brain regions with structural MRI (Amyot et al., 2017). CVR (with fMRI) maps show asymmetries in the chronic TBI population that reliably differentiates them from HC. In areas of visible encephalomalacia on structural MRI, we noted a decrease in CVR. With fNIRS with 16 channels, asymmetric CVR map were also observed and the presence of encephalomalacia in the frontal cortex was associated with low CVR (Fig. 5), an expected finding which provides internal validity to this measure.

Both modalities give statistically different CVR for HC group and TBI group. With fMRI, in our 27 TBI, 20 present visible CVR deficits in the frontal cortex. If we create two subgroups in our TBI population, the TBI subgroup without visible frontal CVR deficits has a CVR much higher (CVR<sub>fNIRS</sub> = 11.1 ± 5.2) than the TBI subgroup with visible CVR deficits in fMRI (CVR<sub>fNIRS</sub> = 8.33 ± 2.0). Moreover, the CVR values with the subgroup showing no CVR deficits in the frontal cortex have a value close to the CVR value obtained in our HC group ( $p = 0.1$ ). From an individual measure perspective, the 16 channel device is able to detect vascular deficits in the prefrontal cortex and, like our previous study in fMRI (Amyot et al., 2017), we detect focal vascular deficits in patients with or without visible structural lesions on the FLAIR. However, due to the multifocal nature of the vascular injury, subjects with TCVI primarily in non-frontal regions, will not be identified with the fNIRS instrument employed in this study, which was limited to the frontal regions.

The two modalities are moderately correlated (Fig. 6), even using the global CVR value measured by fMRI. It was not possible to correlate fNIRS CVR with CVR in the frontal cortex with fMRI, due to the high variance of regional CVR measures. As was shown by Yezhuvath et al. (2009), large inter-subject variations in CVR were observed between ROIs, often manifesting a two-fold difference. The inter-subject variations in CVR are likely not simply noise, but may reflect different global physiologic status in different subjects. A solution to solve this problem is to divide the voxel- or ROI CVR values by the whole brain CVR (Yezhuvath et al., 2009), an approach that is not appropriate in our study due to the multifocal nature of vascular deficits after TBI.

In summary, this study shows that CVR, a dynamic measure of microvascular function, is a sensitive biomarker of TCVI in chronic moderate/severe TBI. CVR can be obtained with fNIRS or fMRI, and each modality has both advantages and disadvantages: fMRI is the gold standard with a high resolution which can be co-localized with any structural images, but NIRS has a better temporal resolution, with a low cost and easily transferred in outpatient facilities. Using fNIRS for CVR measurement shows promise as an adjunct tool in the diagnostic assessment of TBI but also as a predictive and pharmacodynamic biomarker for interventions targeting TCVI.

### Acknowledgments

Work in the authors' laboratory was supported by the Center for Neuroscience and Regenerative Medicine (CNRM), Uniformed Services University of the Health Sciences (USUHS), Bethesda, MD, by the Military Clinical Neuroscience Center of Excellence (MCNCoE), Department of Neurology, USUHS, and by the Intramural Research Program of the National Institutes of Health. The contents of this paper are solely the responsibility of the authors and do not represent the official views of the Department of Defense, CNRM, MCNCoE, or the

## National Institutes of Health.

## References

- Alderliesten, T., De Vis, J.B., Lemmers, P.M., van Bel, F., Benders, M.J., Hendrikse, J., Petersen, E.T., 2014. Simultaneous quantitative assessment of cerebral physiology using respiratory-calibrated MRI and near-infrared spectroscopy in healthy adults. *Neuroimage* 85 (Pt 1), 255–263.
- Amyot, F., Kenney, K., Moore, C., Harber, M., Turtzo, L.C., Shenouda, C.N., Silverman, E., Gong, Y., Qu, B.X., Harburg, L., Lu, H., Wassermann, E., Diaz-Arrastia, R., 2017. Imaging of cerebrovascular function in chronic traumatic brain injury. *J. Neurotrauma*.
- Ayaz, H., 2010. Functional Near Infrared Spectroscopy Based Brain Computer Interface. Drexel University, Philadelphia, PA 2010.
- Ayaz, H., I.M., Shewokis, P.A., Onaral, B., 2010. Sliding-window motion artifact rejection for functional near-infrared spectroscopy. In: Conference Proceedings of the Annual International Conference of the IEEE Engineering in Medicine and Biology Society 2010, pp. 6567–6570.
- Ayaz, H., Shewokis, P.A., Bunce, S., Izzetoglu, K., Willems, B., Onaral, B., 2012. Optical brain monitoring for operator training and mental workload assessment. *Neuroimage* 59, 36–47.
- Bailey, D.M., Jones, D.W., Sinnott, A., Brugniaux, J.V., New, K.J., Hodson, D., Marley, C.J., Smirl, J.D., Ogo, S., Ainslie, P.N., 2013. Impaired cerebral haemodynamic function associated with chronic traumatic brain injury in professional boxers. *Clin. Sci. (Lond.)* 124, 177–189.
- Barkai, G., Goshen, E., Tzila Zwas, S., Dolberg, O.T., Pick, C.G., Bonne, O., Schreiber, S., 2004. Acetazolamide-enhanced neuroSPECT scan reveals functional impairment after minimal traumatic brain injury not otherwise discernible. *Psychiatry Res.* 132, 279–283.
- Bartnik-Olson, B.L., Holshouser, B., Wang, H., Grube, M., Tong, K., Wong, V., Ashwal, S., 2014. Impaired neurovascular unit function contributes to persistent symptoms after concussion: a pilot study. *J. Neurotrauma* 31, 1497–1506.
- Blumbers, P.C., Scott, G., Manavis, J., Wainwright, H., Simpson, D.A., McLean, A.J., 1995. Topography of axonal injury as defined by amyloid precursor protein and the sector scoring method in mild and severe closed head injury. *J. Neurotrauma* 12, 565–572.
- Bonne, O., Gilboa, A., Louzoun, Y., Kempf-Sherf, O., Katz, M., Fishman, Y., Ben-Nahum, Z., Krausz, Y., Bocher, M., Lester, H., Chisin, R., Lerer, B., 2003. Cerebral blood flow in chronic symptomatic mild traumatic brain injury. *Psychiatry Res.* 124, 141–152.
- Chassidim, Y., Veksler, R., Lublinsky, S., Pell, G.S., Friedman, A., Shelef, I., 2013. Quantitative imaging assessment of blood-brain barrier permeability in humans. *Fluids Barriers CNS* 10, 9.
- Chernomordik, V., Amyot, F., Kenney, K., Wassermann, E., Diaz-Arrastia, R., Gandjbakhche, A., 2016. Abnormality of low frequency cerebral hemodynamics oscillations in TBI population. *Brain Res.* 1639, 194–199.
- Cui, X., B.S., Reiss, A.L., 2010. Functional near infrared spectroscopy (NIRS) signal improvement based on negative correlation between oxygenated and deoxygenated hemoglobin dynamics. *Neuroimage* 49, 3039–3046.
- Cui, X., Bray, S., Bryant, D.M., Glover, G.H., Reiss, A.L., 2011. A quantitative comparison of NIRS and fMRI across multiple cognitive tasks. *Neuroimage* 54, 2808–2821.
- Delpy, D.T., Cope, M., van der Zee, P., Arridge, S., Wray, S., Wyatt, J., 1988. Estimation of optical pathlength through tissue from direct time of flight measurement. *Phys. Med. Biol.* 33, 1433–1442.
- Diedler, J., Zweifel, C., Budohoski, K.P., Kasprowitz, M., Sorrentino, E., Haubrich, C., Brady, K.M., Czosnyka, M., Pickard, J.D., Smielewski, P., 2011. The limitations of near-infrared spectroscopy to assess cerebrovascular reactivity: the role of slow frequency oscillations. *Anesth. Analg.* 113, 849–857.
- Furuya, Y., Hlatky, R., Valadka, A.B., Diaz, P., Robertson, C.S., 2003. Comparison of cerebral blood flow in computed tomographic hypodense areas of the brain in head-injured patients. *Neurosurgery* 52, 340–345 discussion 345–346.
- Gardner, A.J., Tan, C.O., Ainslie, P.N., van Donkelaar, P., Stanwell, P., Levi, C.R., Iverson, G.L., 2015. Cerebrovascular reactivity assessed by transcranial Doppler ultrasound in sport-related concussion: a systematic review. *Br. J. Sports Med.* 49, 1050–1055.
- Graham, D., Gennarelli, T., McIntosh, T., 2002. Cellular and molecular consequences of TBI. Graham, D.I., PL, L. (Eds.), *Cellular and molecular consequences of TBI*. Greenfield's Neuropathology 823–898 pps.
- Hasadsri, L., Wang, B.H., Lee, J.V., Erdman, J.W., Llano, D.A., Barbey, A.K., Wszalek, T., Sharrock, M.F., Wang, H.J., 2013. Omega-3 fatty acids as a putative treatment for traumatic brain injury. *J. Neurotrauma* 30, 897–906.
- Huppert, T.J., Hoge, R.D., Dale, A.M., Franceschini, M.A., Boas, D.A., 2006. Quantitative spatial comparison of diffuse optical imaging with blood oxygen level-dependent and arterial spin labeling-based functional magnetic resonance imaging. *J. Biomed. Opt.* 11, 064018.
- Izzetoglu, M., B.S., Izzetoglu, K., Onaral, B., Pourrezaei, K., 2007. Functional brain imaging using near-infrared technology. *IEEE Eng. Med. Biol. Mag.* 26, 38–46.
- Kainerstorfer, J.M., Sassaroli, A., Hallacoglu, B., Pierro, M.L., Fantini, S., 2014. Practical steps for applying a new dynamic model to near-infrared spectroscopy measurements of hemodynamic oscillations and transient changes: implications for cerebrovascular and functional brain studies. *Acad. Radiol.* 21, 185–196.
- Kainerstorfer, J.M., Sassaroli, A., Tgavalekos, K.T., Fantini, S., 2015. Cerebral autoregulation in the microvasculature measured with near-infrared spectroscopy. *J. Cereb. Blood Flow Metab.* 35, 959–966.
- Kassner, A., Roberts, T.P., 2004. Beyond perfusion: cerebral vascular reactivity and assessment of microvascular permeability. *Top Magn. Reson. Imaging* 15, 58–65.
- Kenney, K., Amyot, F., Moore, C., Haber, M., Turtzo, L.C., Shenouda, C., Silverman, E., Gong, Y., Qu, B.X., Harburg, L., Wassermann, E.M., Lu, H., Diaz-Arrastia, R., 2018. Phosphodiesterase-5 inhibition potentiates cerebrovascular reactivity in chronic traumatic brain injury. *Ann Clin Transl Neurol* 5 (4), 418–428.
- Kenney, K., Amyot, F., Haber, M., Pronger, A., Bogoslovsky, T., Moore, C., Diaz-Arrastia, R., 2016. Cerebral vascular injury in traumatic brain injury. *Exp. Neurol.* 275 (Pt 3), 353–366.
- Kim, J., Whyte, J., Patel, S., Avants, B., Europa, E., Wang, J., Slattery, J., Gee, J.C., Coslett, H.B., Detre, J.A., 2010. Resting cerebral blood flow alterations in chronic traumatic brain injury: an arterial spin labeling perfusion fMRI study. *J. Neurotrauma* 27, 1399–1411.
- Kim, J., Whyte, J., Patel, S., Europa, E., Slattery, J., Coslett, H.B., Detre, J.A., 2012. A perfusion fMRI study of the neural correlates of sustained-attention and working-memory deficits in chronic traumatic brain injury. *Neurorehabil. Neural Repair* 26, 870–880.
- Kreplin, U., Fairclough, S.H., 2013. Activation of the rostromedial prefrontal cortex during the experience of positive emotion in the context of esthetic experience. An fNIRS study. *Front. Hum. Neurosci.* 7.
- Langlois, J.A., Rutland-Brown, W., Wald, M.M., 2006. The epidemiology and impact of traumatic brain injury: a brief overview. *J. Head Trauma Rehabil.* 21, 375–378.
- Lee, J.K., Kibler, K.K., Benni, P.B., Easley, R.B., Czosnyka, M., Smielewski, P., Koehler, R.C., Shaffner, D.H., Brady, K.M., 2009. Cerebrovascular reactivity measured by near-infrared spectroscopy. *Stroke* 40, 1820–1826.
- Lewine, J.D., Davis, J.T., Bigler, E.D., Thoma, R., Hill, D., Funke, M., Sloan, J.H., Hall, S., Orrison, W.W., 2007. Objective documentation of traumatic brain injury subsequent to mild head trauma: multimodal brain imaging with MEG, SPECT, and MRI. *J. Head Trauma Rehabil.* 22, 141–155.
- Li, L., Jiang, Q., Zhang, L., Ding, G., Gang Zhang, Z., Li, Q., Ewing, J.R., Lu, M., Panda, S., Ledbetter, K.A., Whitton, P.A., Chopp, M., 2007. Angiogenesis and improved cerebral blood flow in the ischemic boundary area detected by MRI after administration of sildenafil to rats with embolic stroke. *Brain Res.* 1132, 185–192.
- Lu, H., Liu, P., Yezhuvath, U., Cheng, Y., Marshall, O., Ge, Y., 2014. MRI mapping of cerebrovascular reactivity via gas inhalation challenges. *J. Vis. Exp.*
- Menon, D.K., 2006. Brain ischaemia after traumatic brain injury: lessons from 1502 positron emission tomography. *Curr. Opin. Crit. Care* 12, 85–89.
- Mutch, W.A., Ellis, M.J., Graham, M.R., Wourms, V., Raban, R., Fisher, J.A., Mikulis, D., Leiter, J., Ryner, L., 2014. Brain MRI CO2 stress testing: a pilot study in patients with concussion. *PLoS ONE* 9, e102181.
- Mutch, W.A., Ellis, M.J., Ryner, L.N., Ruth Graham, M., Dufault, B., Gregson, B., Hall, T., Bunge, M., Essig, M., Fisher, J.A., Duffin, J., Mikulis, D.J., for The Canada North Concussion Network, a. and for The University Health Network Cerebrovascular Reactivity Research, G., 2016. Brain magnetic resonance imaging CO2 stress testing in adolescent postconcussion syndrome. *J. Neurosurg.* 125, 648–660.
- Naseer N., H.K., 2013. Classification of functional near-infrared spectroscopy signals corresponding to the right- and left-wrist motor imagery for development of a brain-computer interface. *Neurosci. Lett.* 553, 84–89.
- Oppenheimer, D.R., 1968. Microscopic lesions in the brain following head injury. *J. Neurol. Neurosurg. Psychiatry* 31, 299–306.
- Pereira, A.C., Huddleston, D.E., Brickman, A.M., Sosunov, A.A., Hen, R., McKhann, G.M., Sloan, R., Gage, F.H., Brown, T.R., Small, S.A., 2007. An in vivo correlate of exercise-induced neurogenesis in the adult dentate gyrus. *Proc. Natl. Acad. Sci. U S A* 104, 5638–5643.
- Rodriguez Merzagora, A.C., Izzetoglu, M., Onaral, B., Schultheis, M.T., 2014. Verbal working memory impairments following traumatic brain injury: an fNIRS investigation. *Brain Imaging Behav.* 8, 446–459.
- Rodriguez-Baeza, A., Reina-de la Torre, F., Poca, A., Marti, M., Garnacho, A., 2003. Morphological features in human cortical brain microvessels after head injury: a three-dimensional and immunocytochemical study. *Anat. Rec. A Discov. Mol. Cell Evol. Biol.* 273, 583–593.
- Scrimgeour, A.G., Condlin, M.L., 2014. Nutritional treatment for traumatic brain injury. *J. Neurotrauma* 31, 989–999.
- Selb, J., Boas, D.A., Chan, S.T., Evans, K.C., Buckley, E.M., Carp, S.A., 2014. Sensitivity of near-infrared spectroscopy and diffuse correlation spectroscopy to brain hemodynamics: simulations and experimental findings during hypercapnia. *Neurophotonics* 1.
- Shlosberg, D., Benifla, M., Kaufer, D., Friedman, A., 2010. Blood-brain barrier breakdown as a therapeutic target in traumatic brain injury. *Nat. Rev. Neurol.* 6, 393–403.
- Stein, S.C., Chen, X.H., Sinson, G.P., Smith, D.H., 2002. Intravascular coagulation: a major secondary insult in nonfatal traumatic brain injury. *J. Neurosurg.* 97, 1373–1377.
- Taylor, C.A., Bell, J.M., Breiding, M.J., Xu, L., 2017. Traumatic brain injury-related emergency department visits, hospitalizations, and deaths - United States, 2007 and 2013. *MMWR Surveill. Summ.* 66, 1–16.
- Tomlinson, B.E., 1970. Brain-stem lesions after head injury. *J. Clin. Pathol. Suppl. (R. Coll. Pathol.)* 4, 154–165.
- Tong, K.A., Ashwal, S., Holshouser, B.A., Nickerson, J.P., Wall, C.J., Shutter, L.A., Osterdock, R.J., Haacke, E.M., Kido, D., 2004. Diffuse axonal injury in children: clinical correlation with hemorrhagic lesions. *Ann. Neurol.* 56, 36–50.
- Villapol, S., Balarez, M.G., Affram, K., Saavedra, J.M., Symes, A.J., 2015. Neurorestoration after traumatic brain injury through angiotensin II receptor blockage. *Brain* 138, 3299–3315.
- Virtanen, J., Noponen, T., Merilainen, P., 2009. Comparison of principal and independent component analysis in removing extracerebral interference from near-infrared spectroscopy signals. *J. Biomed. Opt.* 14, 054032.
- Wu, H., Jiang, H., Lu, D., Qu, C., Xiong, Y., Zhou, D., Chopp, M., Mahmood, A., 2011. Induction of angiogenesis and modulation of vascular endothelial growth factor receptor-2 by simvastatin after traumatic brain injury. *Neurosurgery* 68, 1363–1371 discussion 1371.

- Yezhuvath, U.S., Lewis-Amezcu, K., Varghese, R., Xiao, G., Lu, H., 2009. On the assessment of cerebrovascular reactivity using hypercapnia BOLD MRI. *NMR Biomed.* 22, 779–786.
- Yezhuvath, U.S., Uh, J., Cheng, Y., Martin-Cook, K., Weiner, M., Diaz-Arrastia, R., van Osch, M., Lu, H., 2012. Forebrain-dominant deficit in cerebrovascular reactivity in Alzheimer's disease. *Neurobiol Aging* 33, 75–82.
- Yuh, E.L., Mukherjee, P., Lingsma, H.F., Yue, J.K., Ferguson, A.R., Gordon, W.A., Valadka, A.B., Schnyer, D.M., Okonkwo, D.O., Maas, A.I., Manley, G.T., Investigators, T.-T., 2013. Magnetic resonance imaging improves 3-month outcome prediction in mild traumatic brain injury. *Ann. Neurol.* 73, 224–235.
- Zhang, F., Signore, A.P., Zhou, Z., Wang, S., Cao, G., Chen, J., 2006. Erythropoietin protects CA1 neurons against global cerebral ischemia in rat: potential signaling mechanisms. *J. Neurosci. Res.* 83, 1241–1251.
- Zhu, Y.S., Tarumi, T., Tseng, B.Y., Palmer, D.M., Levine, B.D., Zhang, R., 2013. Cerebral vasomotor reactivity during hypo- and hypercapnia in sedentary elderly and Masters athletes. *J Cereb Blood Flow Metab* 33, 1190–1196.
- Zweifel, C., Castellani, G., Czosnyka, M., Carrera, E., Brady, K.M., Kirkpatrick, P.J., Pickard, J.D., Smielewski, P., 2010a. Continuous assessment of cerebral autoregulation with near-infrared spectroscopy in adults after subarachnoid hemorrhage. *Stroke* 41, 1963–1968.
- Zweifel, C., Castellani, G., Czosnyka, M., Helmy, A., Manktelow, A., Carrera, E., Brady, K.M., Hutchinson, P.J., Menon, D.K., Pickard, J.D., Smielewski, P., 2010b. Noninvasive monitoring of cerebrovascular reactivity with near infrared spectroscopy in head-injured patients. *J. Neurotrauma* 27, 1951–1958.